LEX LOCALIS-JOURNAL OF LOCAL SELF-GOVERNMENT
ISSN:1581-5374 E-ISSN:1855-363X
VOL. 23, NO. 11(2025)

IMPROVING POWER QUALITY UNDER SECTION 73 OF THE ELECTRICITY ACT, 2003 THROUGH DYNAMIC VOLTAGE RESTORER WITH PROPOSED APPROACH

P.Priyadharshini*[1], Dr.K.Sureshkumar[2]

*[1]Department of EEE, PERI Institute of Technology, Tamilnadu 600048, India.
[2] Department of EEE, Velammal Engineering College, Tamilnadu 600066, India.

*[1]priyadharshini_2007@yahoo.co.in
[2]sureshbarath@gmail.com

Abstract
A number of effects that alter electrical waveforms are arising as a result of the growth of nonlinear loads and electronic gadgets in the distribution network. In order to get over these obstacles, power demand must be satisfied in addition to improving distribution system power quality (PQ) performance. This manuscript presents a hybrid approach for voltage control of a dynamic voltage restorer (DVR). The hybrid technique is the combination of Dung Botox Optimization Algorithm (BOA) and Dual Attention Graph Convolutional Network (DAGCN) and then it is together named as BOA-DAGCN technique. The primary objective is to improve power quality along with DVR in order to achieve a global minimum error and fast dynamic response of the proposed controller. The proposed BOA method is used to optimize the gain parameters of the PI controller. The DAGCN is used to predict the load demand. Finally, the performance of the proposed technique is implemented in MATLAB working platform and compared to various existing approaches. Furthermore, the existing techniques such as Cuckoo search (CSA), Flower pollination Algorithm (FBA), and Grey wolf optimizer (GWO). From the result, the error of proposed method is 1.0936, 1.0158 and 0.1505. The existing CSA is 1.3373, 1.2559 and 0.1324, FBA is 1.4845, 1.3863 and 0.1483 and GWO is 1.5784, 1.4892 and 0.5883.

Keywords: *Current, Dynamic Voltage Restorer, Error, Dung Botox Optimization Algorithm, Power Quality, Voltage sag*

1. Introduction

(a) Background

Energy that is invisible, readily available everywhere in the world, and now acknowledged as a basic consumer necessity is electrical energy [1]. A percentage of the energy demand from sources such as solar, solar thermal, wind, and others is met by Renewable Energy Systems (RESs). The unpredictable nature of harmonics, RESs, and reactive power problems causes the power system to become unstable, which halts the power system's operation [2, 3]. Global distribution grids have extensively adopted Flexible AC Transmission Systems (FACTS) devices to achieve voltage stability, power quality, and reactive power adjustment [4,5]. But FACT devices also alter several aspects of the distribution and transmission systems [6]. PQ problems can manifest in a variety of ways, such as harmonics, interruption, voltage sag/swell, etc. [7]. In distribution networks, voltage sag and swell are the most prevalent PQ problems. The phrase "voltage sag" (either amplitude or phase) refers to a dip in the root mean square voltage (RMS) value at fundamental frequency that lasts from half a cycle to a minute and ranges from 10% to 90% of the nominal voltage [8]. When high-power motors like air conditioners, pumps, and elevators first appeared, it was one of the causes of voltage sag [9–11]. The rise in root mean square voltage (RMS) at fundamental frequency, occurring between 110% and 180% of the nominal voltage, voltage swell is defined as occurring over a half-cycle to a minute. Typically, switching the huge capacitive load is required [12–14]. Voltage sags and swells are often considered disruptions rather than failures or

interruptions [15]. Voltage sag and swell can cause unexpected relay dropouts, adjustable speed drive malfunctions, power converter malfunctions on drives, and other sensitive electrical device failures [16]. The power of electronic gadgets has increased, making the loads in the distribution system more sensitive. These delicate gadgets need to be shielded from several power quality issues, particularly voltage dips. To reduce voltage fluctuations at the load end, a series-connected device called a dynamic voltage restorer (DVR) is utilized [17]. Reactive power correction maintains a consistent voltage profile while active power maintains a constant frequency, as per the power quality standard. Different DVR architectures have developed recently. Multilevel and multicellular topologies have developed from certain topologies [18]. The modular topology of the cascading H-bridge multilevel design is excellent, an easy-to-understand structure, and exceptional hesitant operation ability [19]. More H-bridge modules might be added to expand it to greater voltage levels. The cascaded h-bridge for DVR's five level designs are presented in this paper. The DVR can be operated using a variety of control strategies. The most popular controller is the PI controller, yet in industrial applications, fine-tuning the PI controller's parameters is more challenging. Many alternative controllers have developed during the previous few decades due to the challenges of real-time PI controller parameter tweaking [20]. When the PI controller's transfer function and the reference are both changing in time

(b) Challenges

The system for ensuring quality in the power industry is based on laws written by the government. According to Section 73 of the Electricity Act, 2003, the CEA is responsible for setting technical rules that govern how electricity plants, power lines, and the grid are built, operated, and kept in good condition. This work offers an analysis of power quality, seeks to pinpoint the reasons behind subpar power quality, and offers fixes for these issues. Sensitive equipment includes many items include solid-state electronics, relays, optical devices, laptops, computers, adjustable speed drives, and more. Due to interference from other system components, these components are susceptible to variations in input voltage. Distribution, Transmission, and Generation are the three divisions of the electricity system. Additional transmission lines are used on the distribution side to feed power systems to different loads. When the load is receiving variable power, power quality becomes extremely important in the power system. As a result, the low quality of electricity affects customers who own sensitive loads at home and in businesses. On the distribution side, loads come in a variety of forms, but sensitive loads are more severely damaged by poor power quality than other varieties.

(c) Literature Review

Several research papers that investigate some of the most recent integrated scheduling for dynamic voltage restorer to use a variety of methods and factors to enhance power quality. The following was a review of some of them.

N. Abas *et al.* [21], have presented the power quality (PQ) was a critical issue in the contemporary power system that has an impact on utilities and customers. The combination of smart grid technologies, power electronics technology, and renewable energy sources resulted in a number of problems with the present electric power system. Sensitive equipment can be harmed by voltage sag, swell, current, and voltage harmonics. These components were vulnerable to changes in input voltage brought on by interference from other system components. Because more and more expensive and sophisticated electronic equipment is being used in modern times, power quality has become essential to the power system's ability to operate safely and dependably. The DVR was one possible Distribution D-FACTS instrument that was commonly utilized to resolve

problems. It maintains the voltage profile in the distribution line by injecting voltages to guarantee a constant load voltage. V. Babu *et al*. [22], have presented Voltage swells and sags affected the PQ of the power distribution system. Among other PQ problems, the DVR improved harmonics, voltage sag, and swells. In order to address the power quality issue, the prior Intrinsic Space Vector Transformation (ISVT) control approaches were used in conjunction with the DVR system. It resulted in excessive THD, low efficiency, and steady-state inaccuracy. The SMES-based DVR has done a fantastic job of solving these problems. DVR saves the energy using an alternate energy-using storage mechanism that draws power from a solar PV cell. The MPPT-based P&O algorithm was utilized to balance the solar power. The VSI has to use pulse width modulation (PWM) to make up for the reactive power it generates. Enhancing the reactive power injection into the line also required the feedback control loop. With this rationale, PSVT, a suggested control-based DVR, was put into practice. It examines power variations on the distribution side and produces the appropriate feedback control for the inverter systems. Phase angle mismatch is the outcome of injecting voltage into the line with DVR's help, which gives the grid unsynchronized reactive power. SG has introduced a new control strategy for the electric grid's DVR in the distribution system. Reddy et al. [23]. Voltage sag compensation in the distribution system network and the replacement of the traditional DVR served as the foundation for the suggested DVR employing PI adjusted fuzzy logic scheme. The suggested work was innovative in that it presents a fuzzy logic approach with improved PI tuning that effectively controls the dynamic voltage restorer in cases of rapid voltage sag. The suggested algorithm offers a clever and economical fix for issues with power quality. Our approach was based on closed loop harmonic reduction in the distribution system as well as tailored fuzzy control of reactive powers. In order to reduce power quality difficulties originating from PV-grid side in a hard weather situation, A. Farooqi *et al.* [24] have suggested a technique for improving microgrid stability in a three-phase grid-connected system by adding a dynamic voltage restorer. The most important extreme weather events, like thunderstorms and strong winds, have the potential to cause faults in the transmission network, such as distribution line power outages, lightning strike or impulse transients, and double or single line-to-ground. The suggested method gives the load symmetrical operating conditions and improves the microgrid's transient stability. The error signal was stabilized and the fault signal was extracted by the control mechanism. In order to address power quality concerns, D. Prasad *et al*. [25] have introduced An integrated solar PV DVR uses a rotating dq reference frame controller. The main goal of this study was to create a DVR PI controller that functions effectively and enhance power quality by utilizing an upgraded INC MPPT technique. The Adaptive Neuro-Fuzzy Inference System, or AnFIS, was used to adjust the PI controller. We also performed a mathematical analysis of the suggested solar PV, boost converter, and rotating dq reference frame control. In this project, in addition to using DVR to remove harmonics, swells, and voltage sags, L. Nagarajan et al. [26] have attempted to lessen the prior effects and improve power quality. A DVR that was sensitive enough to satisfy the essential requirements of power quality was suggested; It compensates for inverter drop and modifies the voltage tolerable levels. In this setup, the power supply step-up transformer was connected in series with the DVR-synchronized three-phase voltage, ensuring that the discharge recovery power quality duration and amplitude were appropriate. For the grid system to operate as best it can, the voltage amplitude and phase angle need to be in the right proportion. In the DVR, a series-controlled circuit where the voltage was modified correspondingly, Rational Energy Transformative Optimization Algorithm is devised and used to examine the load variation. This method provides the correct PWM to the VSI, which

generating and absorbing real power or reactive power separately. Recovery line voltages and differential injection voltages have an impact on DVR loads. DVR was an output voltage waveform that has been fine-tuned to produce good power quality, minimal harmonic correction, and mitigation of distribution system voltage transients. A HRES operated by a traditional proportional integral (PI) controller can be connected to the DVR system managed by the adaptive-network fuzzy inference system controller in order to make up for prolonged power quality issues [27]. A solar panel, a PEM fuel cell, and a battery storage device connected to a DC transmission via DC-DC converters make up a HRES. was integrated with DVR architecture in order to harness free and clean energy.

(d) Research Gap and Motivation

The necessity to close current research gaps and improve the efficiency of the technology in DVR development is motivated by lowering distribution network voltage disturbances. Enhancing fault detection and classification capabilities for quicker reaction times, integrating DVRs with smart grid technologies for improved grid resilience and adaptability, developing better control strategies to optimize voltage regulation, and integrating DVRs with renewable energy systems to enhance grid stability are the main areas of ongoing research. Developments in DVR technology can result in more effective, economical, and dependable solutions to enhance electricity quality and make it easier to incorporate renewable energy sources into contemporary distribution networks by addressing certain research gaps and incentives. The drawbacks of existing methods like, CSA may suffer from slow convergence rates and difficulties in balancing exploration and exploitation due to its reliance on randomization. FBA can be sensitive to parameter settings and may struggle with optimization problems that require a high degree of precision due to its simplicity. GWO's performance may deteriorate in complex optimization landscapes with multiple local optima, limiting its effectiveness in solving high-dimensional problems. This work thus supports the DVR control system, a unique contribution to the field, as a low-cost dynamic voltage stabilization scheme. It provides fast dynamic reaction times and little complexity, which enhances power/energy efficiency and improves power quality performance in terms of harmonic reduction and voltage stabilization.

(e) Contribution

- To reduce total harmonic distortion (THD) by taking care of the problem of distorted voltage brought on by swell, sags, or harmonics.
- Examine the power system by introducing harmonics into the input voltage profile..
- The PI controller's gain settings are optimized by the utilization of the proposed BOA approach.. The DAGCN is used to predict the load demand.
- To assess how well the DVR-based power system performs when harmonics are inserted and help improve power quality by fixing voltage sags and swells in the electricity supply.
- With the aid of DVR, access and evaluate the recommended model's performance in MATLAB / Simulink.

(f) Organization

The remaining of the manuscript is expressed as. Sector 2 gives the configuration and analysis of proposed dynamic voltage restorer, Sector 2 displays the proposed methodology, Sector 3 presents the result and discussion and Sector 6 concludes the paper.

2. Configuration and Analysis of Proposed Dynamic Voltage Restorer

One important measure of power quality is the frequency of the supplied voltage, which may be used to determine the quality of the power supply [28]. Complicated activities with a specific

frequency and voltage sag value could maintain the load voltage requirements while causing distortion and oscillation. Voltage sag usually results in downtime and destruction in the industrial sector, which is costly and poses major problems for customers. A certain amount of voltage and electric devices provide current to the distribution system. sometimes referred to as consumer power devices. When it comes to controlling distortion and voltage sag, the DVR is said to be a more efficient solution than more conventional methods. By utilizing a DVR to eliminate voltage sag at the distribution level, the power system's performance is evaluated. Figure 1 depicts the Three-phase DVR system depiction using proposed methodology.

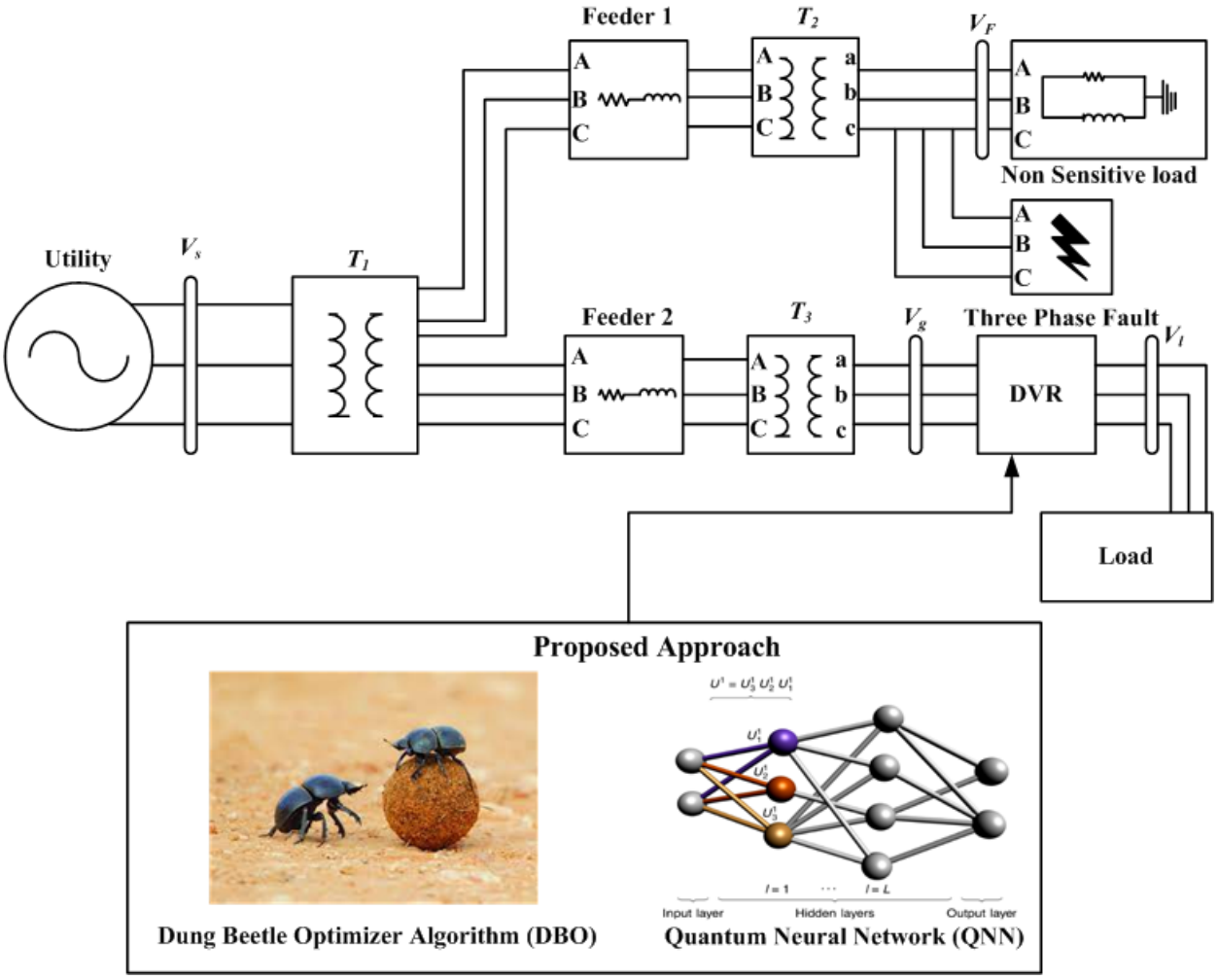

Fig 1: Three-phase DVR system depiction using proposed methodology

Figure 1 illustrates an example study of a distribution system consisting of a utility connected in series with a three-phase, three-winding transformer. Two feeds are linked to the transformer's secondary windings. Feeder and the non-sensitive load-supplying 22/0.38 kV, 500 kVA two-winding transformer are connected to the first feeder. A two-winding transformer that is connected to the other feeder and has 22/0.38 kV, 2 MVA, feeds hybrid load feeders. The proposed BOA-DAGCN approach is connected to the DVR, which is used to improve the power quality.

2.1. Principles and Operation of DVR

The system's venin circuit is shown by its equivalent source impedance (z_S) and voltage source (v_S). It supplies two loads through two feeders (v_f and v_g), where z_{ToT} is the feeder impedance, represented by their respective impedances, z_{l1} and z_{l2} [29]. Under normal operating conditions, Kirchhoff's voltage law (KVL) for a standard DVR is applied to compute the line current (i_S) and the pre-sag voltage ($v_{\Pr e-Sag}$) at the common bus, as exposed in equations (1) and (2):

$$v_{\Pr e-Sag} = v_S - i_S z_s \tag{1}$$

$$i_s = l_1 + l_2 = \frac{v_{\Pr e-Sag}}{z_{ToT} + z_{l2}} + \frac{v_{\Pr e-Sag}}{z_{ToT} + z_{l1}} \tag{2}$$

When the 1st feeder has a fault (f), a high current (i_{SFault}) flows through it. Because of this, equations (3) and (4) provide the common bus voltage during sag

$$v_{Sag} = v_S - i_{SFault}\, z_S \tag{3}$$

$$i_{SFault} = i_1 + i_2 = \frac{v_{Sag}}{z_{ToT}} + \frac{v_{Sag}}{z_{ToT+z_{l1}}} \tag{4}$$

As a result, the injected voltage (v_D) under sag conditions is shown. Equation (5) determines the injected voltage's magnitude and angle. and (6):

$$|v_D| = \sqrt{v_l^2 + v_S^2 - 2v_l v_S Cos(\varphi_l - \theta_S)} \tag{5}$$

$$\phi_d = Tan^{-1}\left(\frac{v_l Sin\phi_l - v_S Sin\phi_S}{v_l Cos\phi_l - v_S Cos\phi_S}\right) \tag{6}$$

In order to increase the load voltage, a portion of the feeders' line reactance is suppressed using series compensation.

2.2. Voltage Sag Indices

To assess the voltage quality of the system, three sag indices are employed to display the DVR correction capabilities [29]. These indices must be easy to use and sensitive to any disruption in order to precisely analyze the system performance. The following is an expression for these indices:

2.2.1. Voltage sag lost energy index (VSLEI)

This catalogue, provided by equation (7), represents the energy lost through a sag situation.

$$w = t\left[1 - \frac{v}{v_{Nom,}}\right]^{\alpha} \tag{7}$$

Where, v_{Nom} is indicated as the nominal voltage, t is the sag time in milliseconds, and v is denoted as the per unit phase voltage. It should be mentioned that the power acceptance curve is the source of factor α.

2.2.2. Sag score (SS) Index

As provided by equation (8), the sag score (SS) is defined as follows:

$$SS = \frac{v_a + v_b + v_c}{3} \quad (8)$$

Where, v_a, v_b, and v_c show the phase voltages at rms.

2.2.3. Voltage Sag Energy (EVS)

The definition of the voltage sag energy is provided by equation (9).

$$E_{VS} = \int_0^t \left\{ 1 - \left(\frac{v(T)}{v_{Nom}} \right)^2 \right\} dt \quad (9)$$

Where t is the length of the sag and V(t) indicates the voltage magnitude at time T, v_{Nom} as normalization of voltage .

2.3. Mathematical Modeling of Dynamic Voltage Restorer with Power Quality

PQ refers to the continuous supply and voltage characteristics (waveform, symmetry, magnitude, frequency, and frequency) of the power supply under typical operating conditions. Power quality problems are divided into four categories: transients, voltage flickers, waveform distortion, imbalanced voltage, and short- and long-term voltage shifts. When the voltage RMS value deviates from the average value for less than a minute, there is a short-duration voltage variation. Harmonics in the distribution system cause a number of negative outcomes, such as overloading and overheating a transformer and rotating machinery [28].

The load (active) power as pl and $vlil$ is denoted as the load absorbed is as follows in eqn (9):

$$pl = vlilCos\theta \quad (9)$$

Where, p_{DVR} is the DVR's active power is provided by equation (10).

$$p_{DVR} > 0 \quad (10)$$

When the DVR uses active power

$$p_{DVR} < 0 \quad (11)$$

When there is no exchange of active power

$$p_{DVR} = 0 \quad (12)$$

There is no active power exchange to compensate for the voltage surge when the voltage limitations are broken. In contrast, in the event of a voltage drop, the device supplies the active power. If the voltage sag is too large to meet the necessary voltage, the injection voltage will be as follows.

$$v_{inj} > \sqrt{v_S^2 + v_l^2 - 2v_S v_l Cos(\theta_S - \theta_L)} \quad (13)$$

From the above equation, v_{inj} is denoted as injection voltage, vs and vl are denoted as voltage source and voltage load

The transmission line of the test system is connected to the DVR system via a three-phase injection transformer.

2.4. Objective Function

Equation (14), which provides the gains of the objective function, may be used to fine-tune the suggested DVR.

$$Min(j) = Min(ITAE) \quad (14)$$

Here, $ITAE$ is indicated as the integral time absolute error and j is denoted as the total error of the proposed DVR's controller [30]. Equation (15) provides the mathematical expression for the $ITAE$ performance index.

$$ITAE = \int_0^\infty T\left|E_T, dq0\right|dt \tag{15}$$

Here $E_T, dq0$ stands for the error signal in the $dq0$ elements positioned between the load and reference voltages. The optimization problem is subject to the following restrictions.

2.5. Constraints

Equation (16) limits the second feeder's voltage level between its lowest and highest values.

$$0.95 \le v_l \le 1.05 \tag{16}$$

Equation (17) indicates that the second feeder's THD of voltage (THD_V) should be less than its maximum value $(THD_{V,Max})$.

$$THD_V = \frac{\sum_{H=2}^{N} V_H^2}{v_1} \tag{17}$$

$$THD_V \le THD_{V,Max} \tag{18}$$

3. Proposed BOA-DAGCN Based Community Integrated Energy Systems

The BOA-DAGCN is used to tune the controller gains for DVR in order to maximize power quality performance with respect to different voltage profile issues, including balanced and unbalanced sag/swell, voltage imbalance, notching, and different fault conditions, as well as power system harmonic distortion mitigation. To be stable and respond adequately to various shocks, the chosen gains reduce the error signal. Thus, to enhance overall performance, the fitness function with the lowest error is chosen. The following illustrates the suggested approach's detailed explanation:

3.1. Optimization of Botox Optimization Algorithm (BOA)

The BOA is an optimization metaheuristic that takes its cues from the way botulinum toxin, also referred to as "Botox," works [31]. BOA focuses on iteratively refining a population of solutions by selectively analyzing less viable portions of the search space and allowing potential regions to grow, much like Botox injections targets certain muscles to accomplish desired cosmetic effects. This is done by combining exploration and exploitation techniques in such a way that solutions with lower fitness values are suppressed and better solutions are encouraged to spread. Solutions are evaluated based on their fitness. By dynamically adjusting the balance between exploration and exploitation, BOA effectively navigates complex optimization landscapes and converges towards high-quality solutions across various problem domains. The flowchart of BOA is shown in fig 2.

Step 1*: *Initialization

Set the input parameters to their initial values (current and voltage in this case).

Step 2*: *Random Generation

After setup, the random vectors generate the input factors at arbitrary.

$$R = \begin{bmatrix} R_{1.1} & R_{1.2} & \dots & R_{1.x} \\ R_{2.1} & R_{2.2} & \dots & R_{2.x} \\ \dots & \dots & \dots & \dots \\ R_{y.1} & R_{y.2} & \dots & R_{y.x} \end{bmatrix} \quad (28)$$

Where, y is the number of variable and x is the number of dimension in the solution space.

Step 3*: *Fitness Function

Fitness is based on the objective function,

$$F = MIN(j) \quad (29)$$

j is denoted as the total error

Step 4: Exploration Phase

The capacity of the algorithm to efficiently investigate a collective group may be evaluated and adjusted by measurement of the BOA population diversity. This measure basically tells us if the population members are concentrating on exploring. Population diversity of the BOA refers to how the population is distributed within the issue space, and it is important to note this for tracking the algorithm's search activities.

$$Exploration = \frac{\frac{1}{N}\sum_{i=1}^{N}\sqrt{\sum_{d=1}^{m}\left(x_{i,d} - \bar{x}_d\right)^2}}{\frac{1}{N}\sum_{i=1}^{N}\sqrt{\sum_{d=1}^{m}\left(x_{i,d} - \bar{x}_d\right)^2}_{\max}} \quad (30)$$

Where x_d is represented as the population mean in the d dimension, N is denoted as the quantity of population members, and m is indicated as the quantity of issue dimensions.

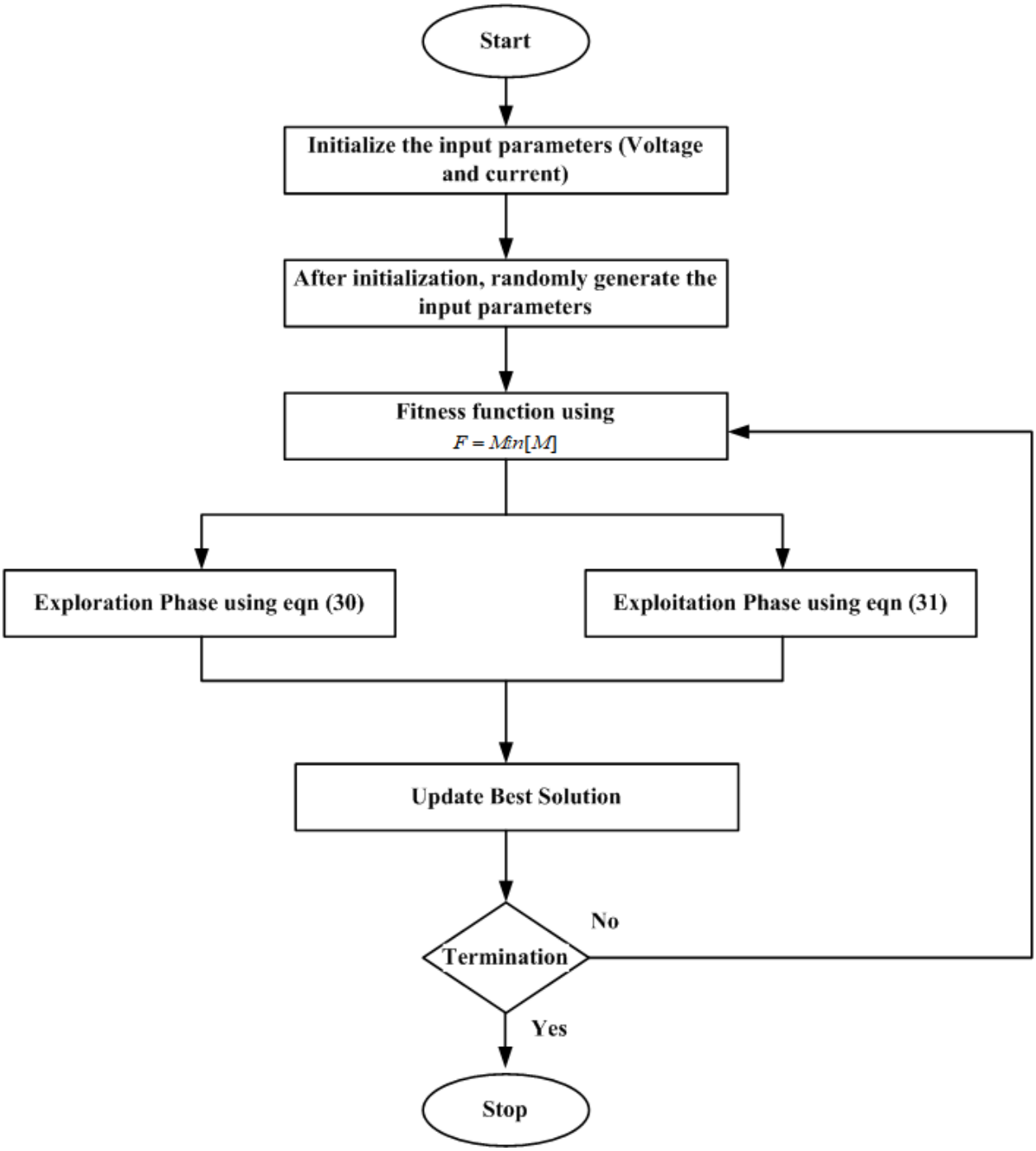

Fig 2: Flowchart of BOA

Step 5: Exploitation phase

Equation may be used to define the population exploitation percentage for each iteration.

$$Exploitation = 1 - \frac{1}{N}\sum_{i=1}^{N}\sqrt{\sum_{d=1}^{m}\left(x_{i,d} - \bar{x}_d\right)^2} \quad (31)$$

23 standard benchmark functions are used to evaluate the examination of exploration, exploitation, and population diversity —seven of which are unimodal and sixteen multimodal which are given in this subsection.

Step 6: Update the Best Solution

After updating the condition in light of the first and second stages, the BOA iteration is said to be finished.

Step 7: Termination

If the solution is the best, the procedure gets terminated; if not, it goes back to step 3 fitness evaluations and continue processing the next stages until a solution is found.

3.2. Dual Attention Graph Convolutional Network (DAGCN)

The DAGCN can be used to predict the load and focusing on reducing error and improving the power quality [32]. The three main components of the DAGCN are the fully connected classifier, the self-attention pooling layer, and the attention graph convolution module, as mentioned in reference. We first discuss the problems with conventional Graph Convolutional Networks (GCNs) in this part, and then we present our new self-attention pooling layer and attention graph convolution module. The following expression can be used to calculate the convolutions of the system:

$$W^{j+1} = \phi(\widetilde{V}\widetilde{D}^{-1}W^{j}U) \quad (31)$$

Where, $\widetilde{V}$'s are represents relating to the node degree matrix diagonal, $\widetilde{D}$ and $\widetilde{V}\widetilde{D}^{-1}$ is denotes to the normalized graph structure, $\widetilde{V} = V + I_m$ is refers to the adjacency matrix for every node that includes self-connections and U is specifies to the model factor to be trained. After performing this process j times, W^j becomes a node attributes vector containing H-hop local structure information.

Every step's result throughout the replication of the concession of W^j can only be used to produce the following convolution result. Enhancing the model's dependence on the k-hop convolution result is the main objective of the AGC layer, which also aims to extract useful information from each hop. The convolution output will be a logical arrangement of the most relevant data gathered from the various hop convolution operations. Demonstrate the attention behavior and apply it to the following hierarchical node representation (γ_{s_m}):

$$\gamma_{s_m} = \sum_{k=1}^{j} \alpha_{ki} W_{s_m}^{j} \quad (32)$$

To make things easier, consider the vanilla factor while determining the significance of each hop's aggregation result: α stands for the attention weight, and $W_{s_m}^{j}$ is a node s_m that determines the local structure in j-hops. Details on the hierarchical structure are included in the final node representation.

$$\gamma_{s_m}^{n+1} = \sum_{k=1}^{j} \alpha_k W_{s_m}^{j} \quad (33)$$

$$W_{s_m}^{0} = \gamma_{s_m}^{n} + Y \quad (34)$$

Using the residual learning approach to construct an attention graph convolutional module and stacking attention convolution layers enables us to access deeper hidden features and use the

benefits of deep learning. With this approach, the final node representation as γ_{s_m} is intended to be greatly improved. The output from the layer before it and the original Y make up each AGC layer's input.

$$\gamma_{s_m} = Dense\ (\{\gamma_{s_m}^0, \gamma_{s_m}^1, ..., \gamma_{s_m}^n\}, \theta) \quad (35)$$

Where the outputs of every attention graph convolutional layer are combined by a dense layer called $Dense$. Now, all vertices $s \in Q$ have a node representation of γ. For simplicity, consider the graph to be a matrix Q of size m by c, with each row representing a node.

$$Q = (\gamma_{s_1}, \gamma_{s_2}, \ldots, \gamma_{s_m}) \quad (36)$$

To output the weights vector α, use the attention mechanism with the convolution module's graph node representation as the input.

$$\beta = soft\max(h_2 \tan w(h_1 Q^T)) \quad (37)$$

Where, h_1 and h_2 are c-by-r and c-by-c weight matrices, correspondingly, and r is indicated as a hyper-parameter that controls how many reflecting subspaces are utilized to estimate the graph representation of the node demonstration. When $r \geq 1$ and α are combined, they yield a matrix with weights rather than a vector.

Graph illustration the matrix in which each column represents an illustration in one subspace, and a thorough depiction of the graph is generated by the complete matrix. A fully connected layer and a $soft\max$ layer, which accepts G as input, come next to finish the graph categorization.

$$X = soft\max(ZG + C) \quad (38)$$

Where, the second input dimension is used to conduct the $soft\max$ function.

3. Result and Discussion

The MATLAB platform is used to analyze the supplied DVR in terms of optimizing voltage sag and swell, both balanced and unbalanced, as well as various failure scenarios, voltage imbalance, voltage notching, and transient conditions for the power system. The current and voltage results are shown and both the simulations with and without the suggested DVR are included. Additionally, the method is contrasted by using the best solution of the benefits from the optimum DVR performance for the error-driven PI controllers.

Fig 3 shows The Sag mode with DVR is displayed. The uncompensated load voltage is shown in volts in subplot (a), while the adjusted load current is shown in subplot (b). There is a three-phase overload applied between t=0.1 and t=0.15 seconds. Additionally, t=0.185 s and t=0.2 s are the periods at which a three-phase induction motor is started. An equilibrium voltage sag mode results from this. The load point's current sag is around 50% and 70%, respectively, with regard to the reference voltage. The DVR raises the load voltage profile of the system by injecting the necessary voltage on the three phases, as can be seen when it is shown during this event, as seen in Fig. 3. Fig 4 shows the sag mode by employing the voltage injection's DVR. Here the three phases of injected voltage flows from -2.5V to 2.9V at the time period of 0sec then it remain constant at 0v at the period of time of 0.05 to 0.2 sec. then three phases of injected voltage flows from -1V to 1V at the time period of 0.2 to 0.3sec then it remain constant at 0v at the time period of 0.3 to 0.4 sec. Fig 5 displays the Uncompensated load voltage in volts (a) and adjusted load current (b) are used in the unbalanced sag mode with DVR is presented. In subplot (a) uncompensated load voltage in volts is presented. The voltage flows from -1V to 1V at the time period of 0 to 0.2sec then at the

period of time of 0.2 to 0.4sec the voltage flows from -1.1V to 1.1V. In subplot (b) compensated load current is presented. Here the load current flows from -1A to 1A at the time period of 0 to 0.5sec. Fig 6 shows the unbalanced sag mode by using DVR of injected voltage. Here the voltage flows from -2.5v to 2.9V at the time period of 0sec then at the period of time of 0.2V to 0.4V the voltage flows from -1.5V to 1.5V.

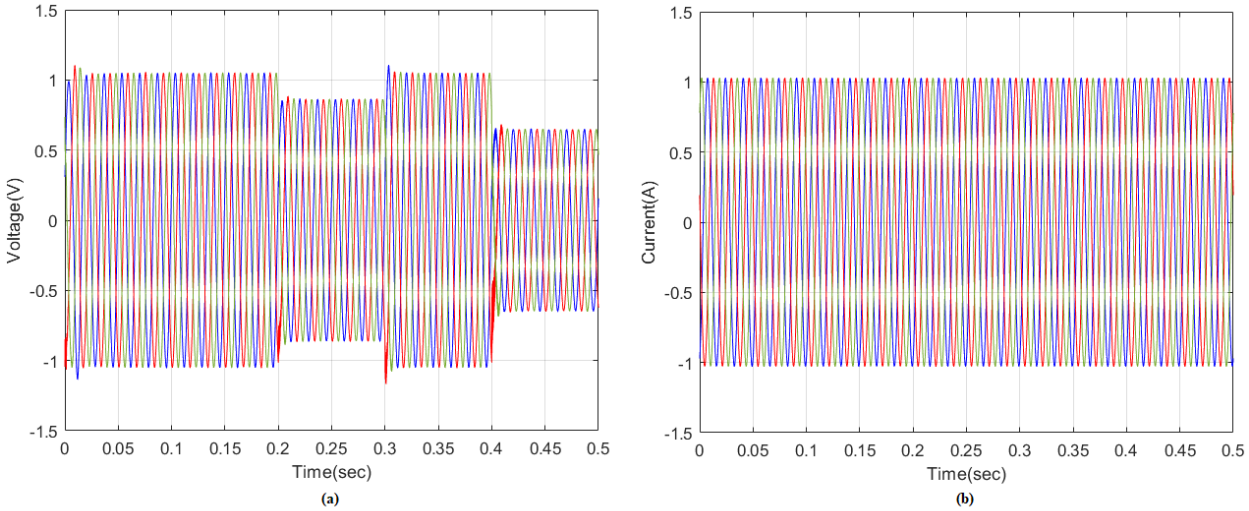

Fig 3: Utilizing DVR to enable sag mode: (a) uncompensated load voltage in volts; (b) compensated load current

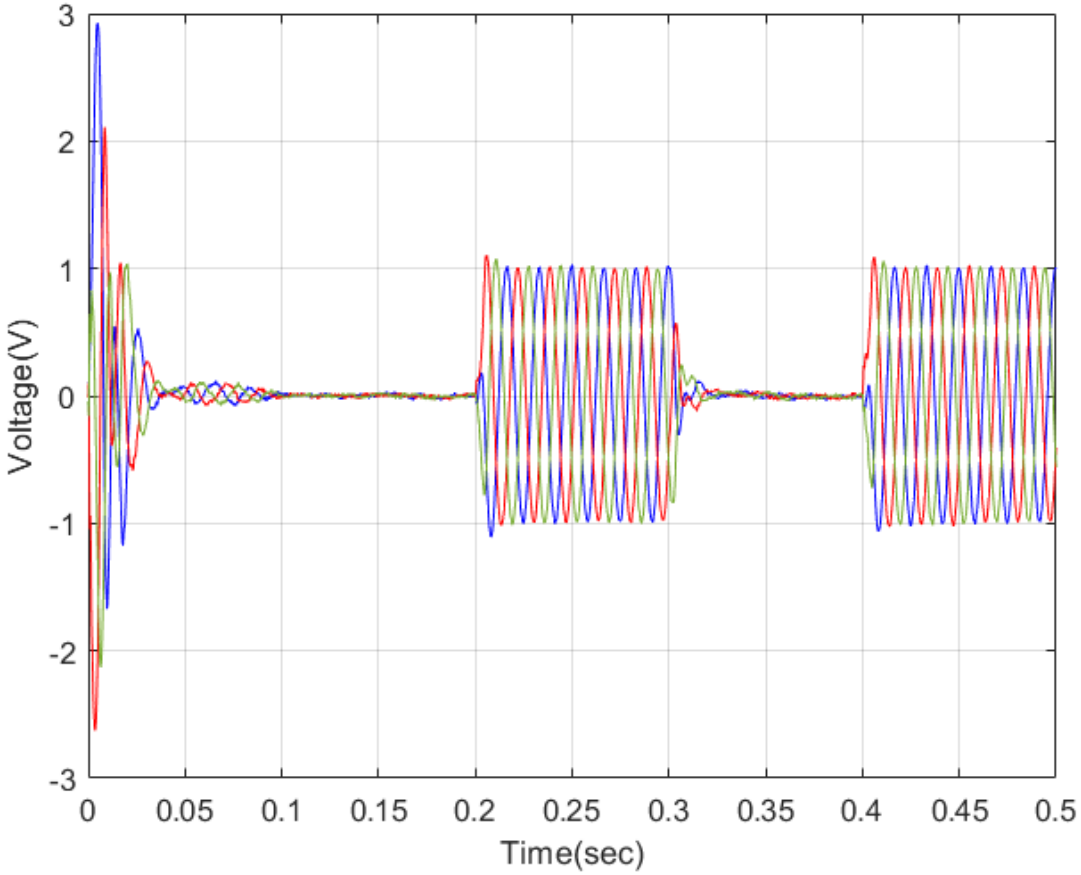

Fig 4: Sag mode by employing the voltage injection's DVR.

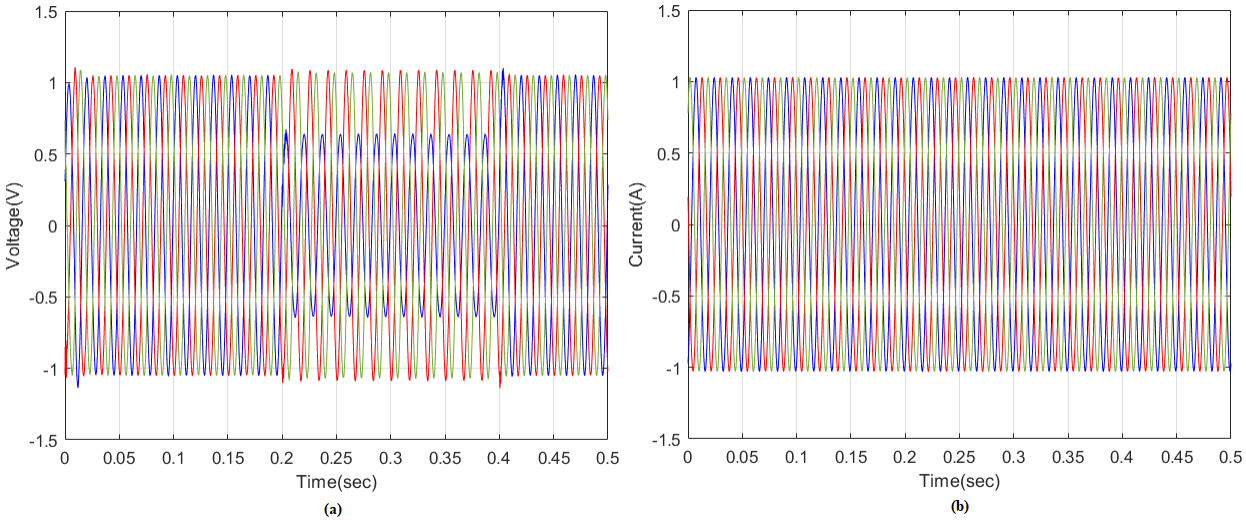

Fig 5: Uncompensated load voltage in volts (a) and adjusted load current (b) are used in the unbalanced sag mode with DVR.

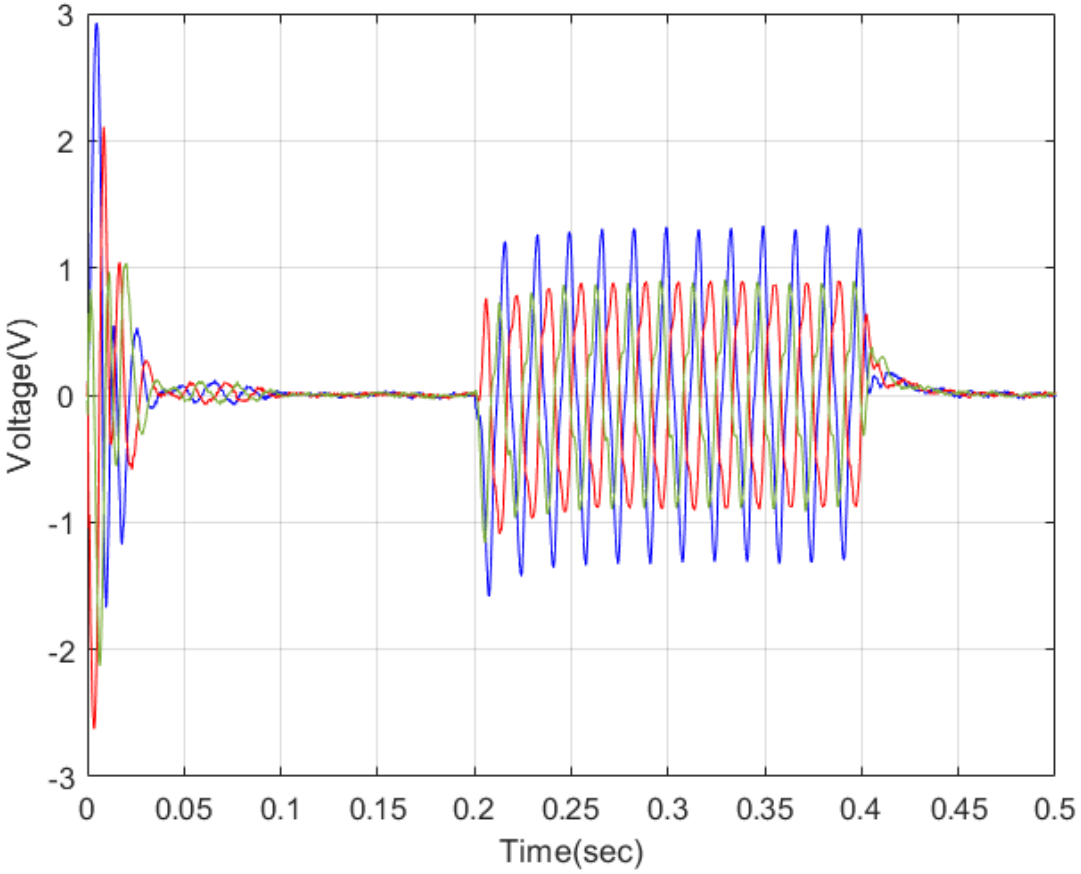

Fig 6: Unbalanced sag mode by using DVR of injected voltage

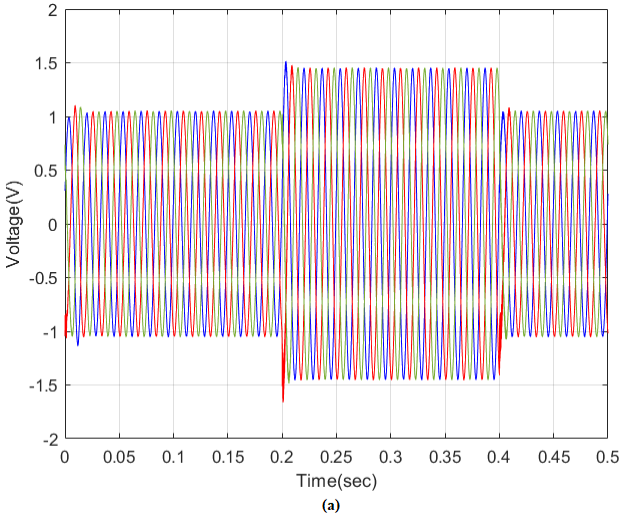

(a)

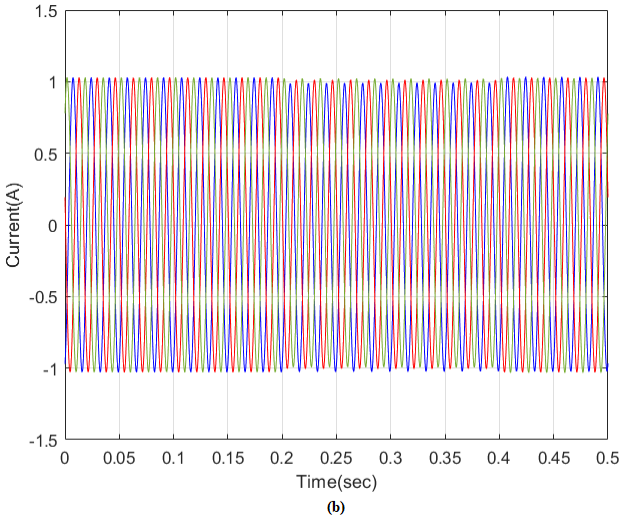

(b)

Fig 7: Using DVR to provide balanced swell mode: (a) load voltage in volts without compensation, (b) load current with compensation

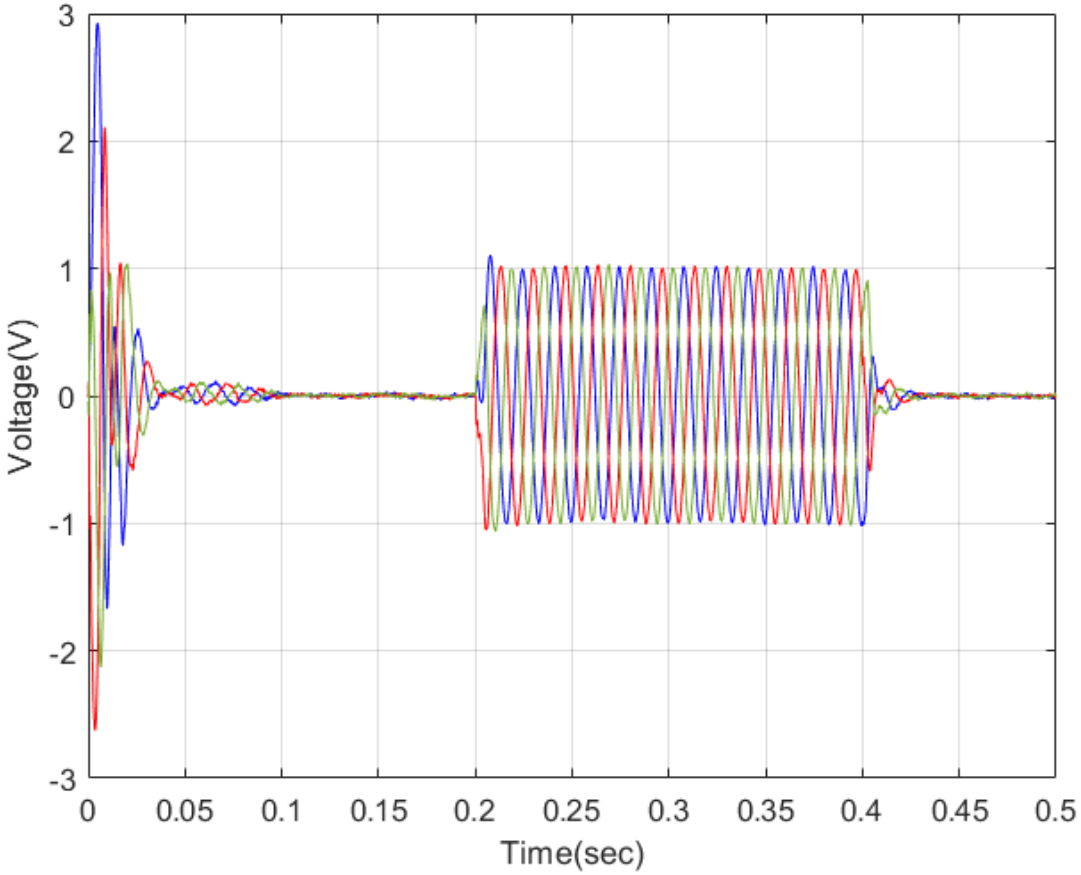

Fig 8: Balanced swell mode by using DVR of injected voltage

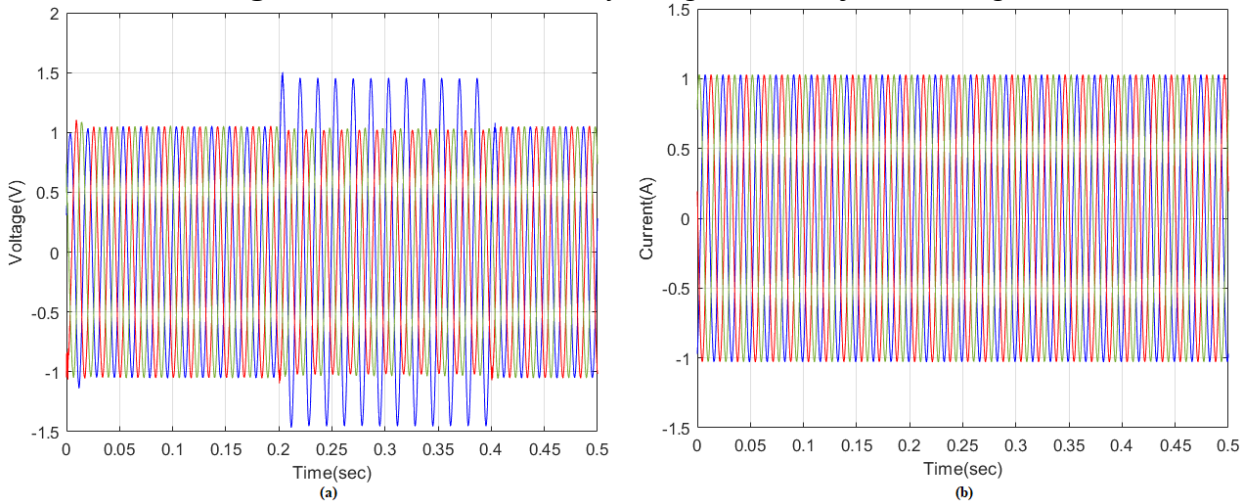

Fig 9: Uncompensated load voltage in volts (a) and adjusted load current (b) in unbalanced swell mode with DVR

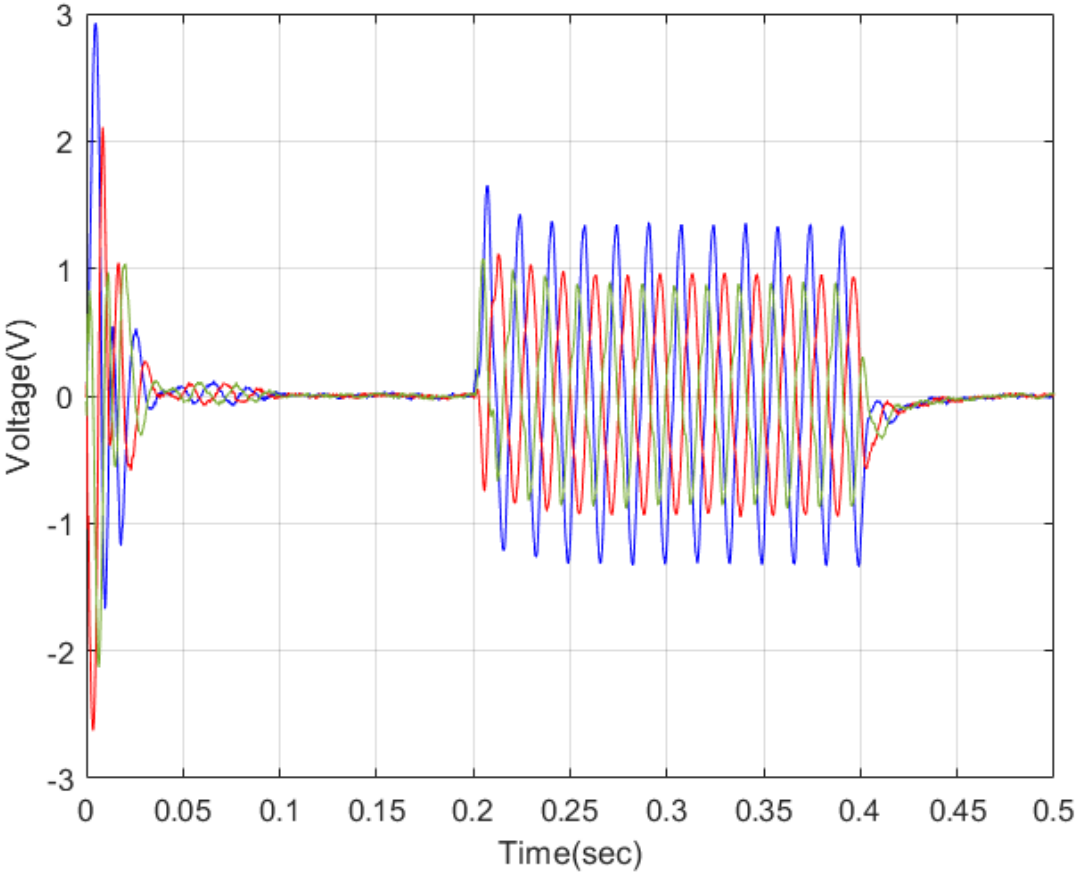

Fig 10: Unbalanced swell mode by using DVR of injected voltage

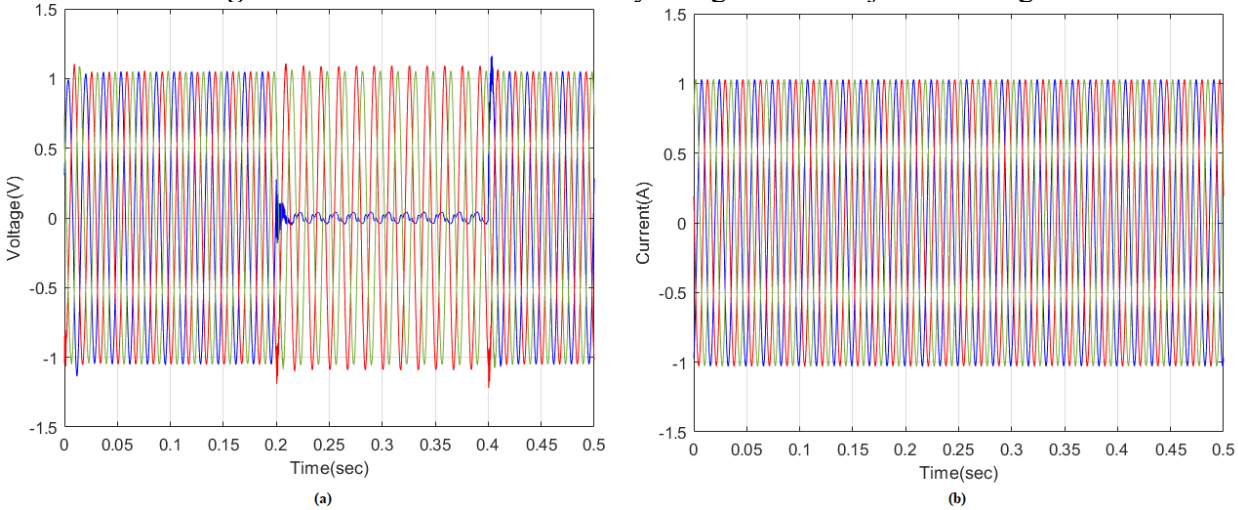

Fig 11: Single line to ground fault enabled via DVR: (a) a volt-measured faulty feeder; (b) an uncompensated load current

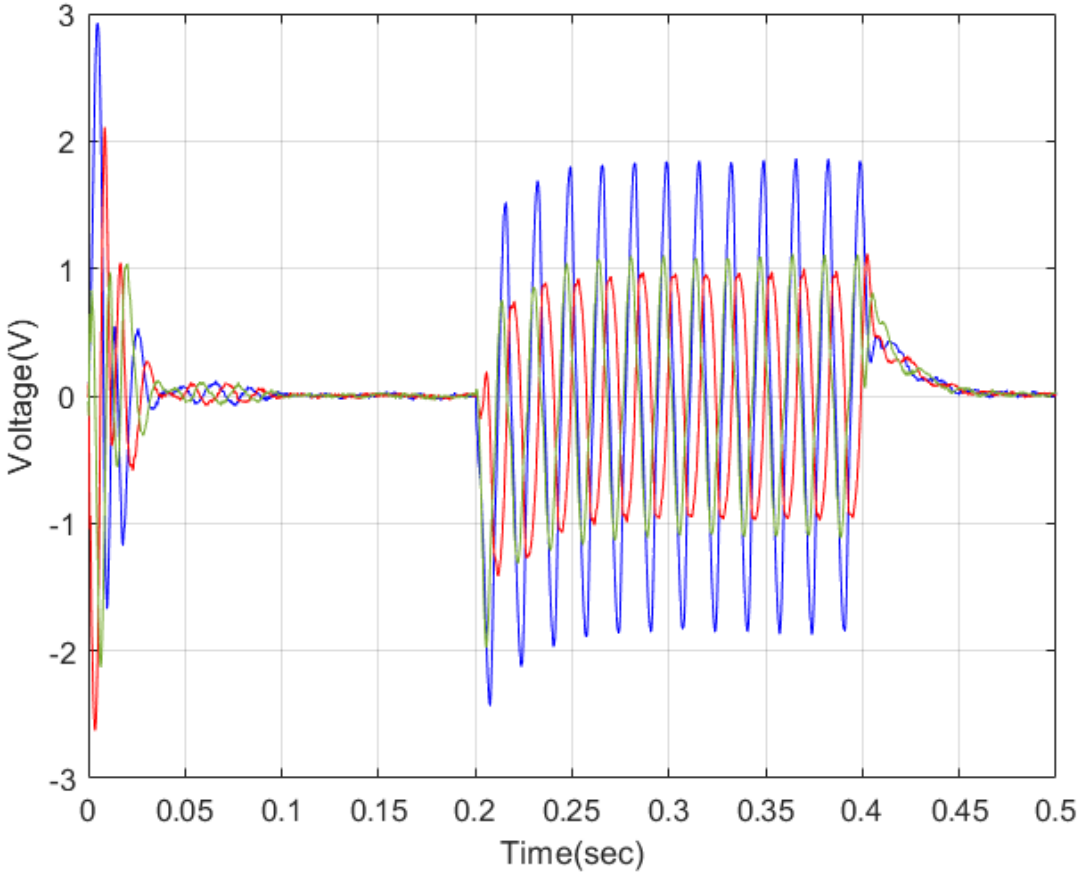

Fig 12: Single line to ground fault using DVR of injected voltage

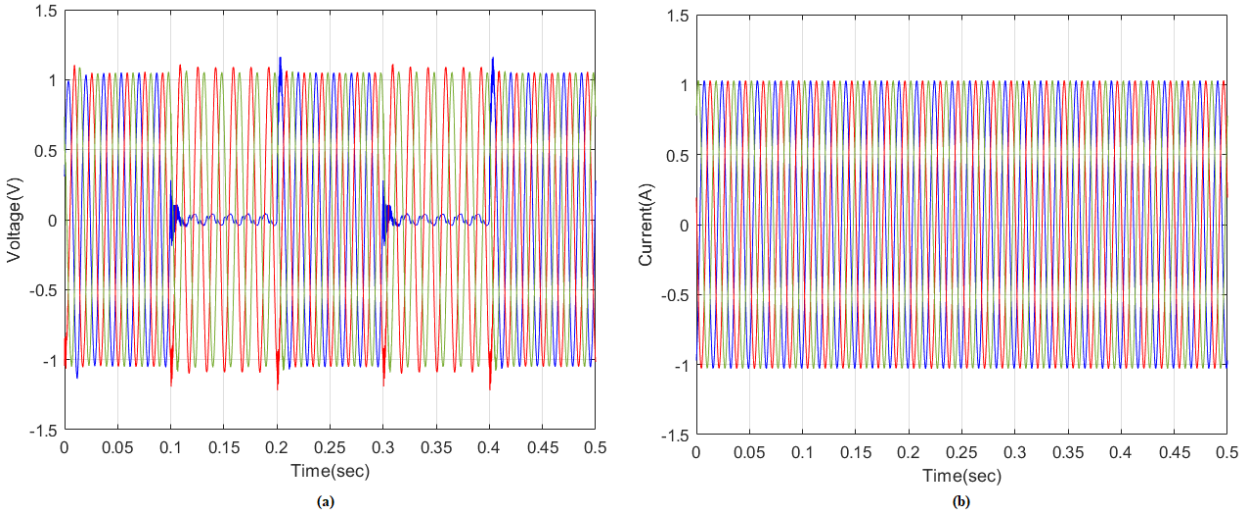

Fig 13: Utilizing DVR to measure voltage imbalance, (a) uncompensated load voltage in volts, and (b) compensated load current

Fig 7 shows Using DVR to provide balanced swell mode: (a) load voltage in volts without compensation, (b) load current with compensation is presented. In subplot (a) uncompensated load voltage in volts is presented. The voltage flows from -1V to 1V at the time period of 0 to 0.2sec then at the period of time of 0.2 to 0.4sec the voltage increased from -1.5V to 1.15V. In subplot (b) compensated load current is presented. Here the load current flows from -1A to 1A at the time period of 0 to 0.5sec. Fig 8 shows the balanced sag mode by using DVR of injected voltage. Here the voltage flows from -2.5v to 2.9V at the time period of 0sec then at the period of time of 0.2V to 0.4V the voltage flows from -1.V to 1.V. Fig 9 shows Uncompensated load voltage in volts (a) and adjusted load current (b) in unbalanced swell mode with DVR is presented. In subplot (a) uncompensated load voltage in volts is presented. The voltage flows from -1V to 1V at the time period of 0 to 0.2sec then at the period of time of 0.2 to 0.4sec the voltage increased from -1.5V to 1.15V. In subplot (b) compensated load current is presented. Here the load current flows from -1A to 1A at the period of time of 0 to 0.5sec. Fig 10 shows the unbalanced sag mode by using DVR of injected voltage. Here the voltage flows from -2.5v to 2.9V at the time period of 0sec then at the period of time of 0.2V to 0.4V the voltage flows from -1.V to 1.V. Fig 11 shows the Single line to ground fault enabled via DVR: (a) a volt-measured faulty feeder; (b) an uncompensated load current is presented. The voltage flows from -1V to 1V at the time period of 0 to 0.2sec then at the period of time of 0.2 to 0.4sec the voltage increased from -1.1V to 1.11V. In subplot (b) uncompensated load current is presented. Here the load current flows from -1A to 1A at the period of time of 0 to 0.5sec. Fig 12 shows the unbalanced sag mode by using DVR of injected voltage. Here the voltage flows from -2.5v to 2.9V at the time period of 0sec then at the period of time of 0.2V to 0.4V the voltage flows from -1.V to 1.V. Fig 13 shows the Utilizing DVR to measure voltage imbalance, (a) uncompensated load voltage in volts, and (b) compensated load current is presented. The voltage flows from -1V to 1V at the time period of 0 to 0.1sec then at the period of time of 0.1 to 0.2sec the voltage increased from -1.5V to 1.15V. In subplot (b) compensated load current is presented. Here the load current flows from -1A to 1A at the time period of 0 to 0.5sec.

Table 1: THD analysis before and after compensation [28]

Analysis	THD	Load voltage(V)	Load Current (A)
Uncompensated Voltage	1.58	217.1	54.6
Compensated Voltage	0.702	218.3	17.45

Table 2: A statistical analysis of existing and proposed systems [28]

Solution Techniques	Mean	Median	SD
Proposed	1.0936	1.0158	0.1505
CSA	1.3373	1.2559	0.1324
FBA	1.4845	1.3863	0.1483
GWO	1.5784	1.4892	0.5883

Table 1 shows the THD analysis before and after compensation with load voltage and current of uncompensated and compensated voltage. Table 2 shows the A statistical analysis of existing and proposed systems [28]. The proposed method is 1.0936, 1.0158 and 0.1505. The existing CSA is 1.3373, 1.2559 and 0.1324, FBA is 1.4845, 1.3863 and 0.1483, GWO is 1.5784, 1.4892 and 0.5883.

3.1. Discussion

When there are balanced three-phase voltage sags between t=0.2 and t=0.3 seconds, they are known as balanced voltage sags, the controllers' performance is evaluated using a PI. There is a 30% decrease in voltage. These numbers show that the model's performance with the ideal PI controller outperforms the performance achieved with the optimal PI controller, it raises the voltage back to 99%. The measured values obtained from ITAE were 1.325 and 0.813, respectively. The voltage source inverter's switching signal is driven by the DVR scheme, which is managed by an optimal PI regulation controller. With the goal of reducing the overall error-driven loop and ensuring a quick, dynamic reaction for efficient energy use, this technique ascertains the optimal fitness value.

4. Conclusion

In this study, a hybrid method for DVR voltage regulation is presented. The main goal is to enhance power quality in conjunction with DVR so that the proposed controller may achieve a global minimal error and quick dynamic response. By using the proposed BOA technique, the gain parameters of the PI controller are improved. The DAGCN is used to predict the load. To demonstrate the efficacy of control algorithms, the internal signals of every control algorithm are shown in the event of supply voltage distortions and voltage sag. Lastly, the proposed technique's performance is put into practice using the MATLAB working platform, and its results are contrasted with those of other existing approaches. The outcomes demonstrated the optimum PI controller's improved efficacy and resilience. From the result, the error of proposed method is 1.0936, 1.0158 and 0.1505. The existing CSA is 1.3373, 1.2559 and 0.1324, FBA is 1.4845, 1.3863 and 0.1483 and GWO is 1.5784, 1.4892 and 0.5883.

4.1. Limitation

- One of the main limitations of dynamic voltage restorers (DVRs) is their relatively high initial cost, which can be a barrier to widespread adoption, especially for smaller distribution system operators or end-users.
- DVRs can be bulky and require specific installation considerations, such as adequate space and cooling requirements, which may pose challenges in retrofitting existing systems or integrating them into constrained spaces.
- DVRs require regular maintenance to ensure optimal performance, and servicing these devices may require specialized technical expertise, leading to additional operational costs and potential downtime.
- DVRs have a limited coverage area, and deploying multiple units to cover a larger distribution network can be complex and costly, making it challenging to provide comprehensive voltage support across the entire grid.

4.2. Future Scope

- There is potential to integrate energy storage systems with DVRs to enhance performance and support renewable energy integration in the grid.
- Future DVR technologies will prioritize cyber security measures to ensure the reliability and grid operations' security in the face of growing digitalization.
- The idea of using multiple smaller DVR units across the distribution network may become more common to improve voltage quality and grid stability.
- Future DVRs may have the ability to interact with other grid assets like smart inverters, enabling more coordinated voltage control strategies for a more resilient power distribution system.

Reference

[1] Mahmoud, M.M., Esmail, Y.M., Atia, B.S., Kamel, O.M., AboRas, K.M., Bajaj, M., Hussain Bukhari, S.S. and Mbadjoun Wapet, D.E., 2022. Voltage quality enhancement of low-voltage smart distribution system using robust and optimized DVR controllers: Application of the Harris hawks algorithm. *International Transactions on Electrical Energy Systems*, *2022*.

[2] Shah, M.S., Mahmood, T., Ullah, M.F., Manan, M.Q. and Rehman, A.U., 2022. Power quality improvement using dynamic voltage restorer with real twisting sliding mode control. *Engineering, Technology & Applied Science Research*, *12*(2), pp.8300-8305.

[3] Pal, R. and Gupta, S., 2020. Topologies and control strategies implicated in dynamic voltage restorer (DVR) for power quality improvement. *Iranian Journal of Science and Technology, Transactions of Electrical Engineering*, *44*, pp.581-603.

[4] Moghassemi, A. and Padmanaban, S., 2020. Dynamic voltage restorer (DVR): a comprehensive review of topologies, power converters, control methods, and modified configurations. *Energies*, *13*(16), p.4152.

[5] DaneshvarDehnavi, S., Negri, C., Bayne, S. and Giesselmann, M., 2022. Dynamic Voltage Restorer (DVR) with a novel robust control strategy. *ISA transactions*, *121*, pp.316-326.

[6] Farooqi, A., Othman, M.M., Radzi, M.A.M., Musirin, I., Noor, S.Z.M. and Abidin, I.Z., 2022. Dynamic voltage restorer (DVR) enhancement in power quality mitigation with an adverse impact of unsymmetrical faults. *Energy Reports*, *8*, pp.871-882.

[7] Awaar, V.K., Jugge, P., Kalyani, S.T. and Eskandari, M., 2023. Dynamic voltage restorer–a custom power device for power quality improvement in electrical distribution systems. In *Power Quality: Infrastructures and Control* (pp. 97-116). Singapore: Springer Nature Singapore.

[8] Molla, E.M. and Kuo, C.C., 2020. Voltage sag enhancement of grid connected hybrid PV-wind power system using battery and SMES based dynamic voltage restorer. *IEEE Access*, *8*, pp.130003-130013.

[9] Chen, X., Xie, Q., Bian, X. and Shen, B., 2021. Energy-saving superconducting magnetic energy storage (SMES) based interline DC dynamic voltage restorer. *CSEE Journal of Power and Energy Systems*, *8*(1), pp.238-248.

[10] Ghavidel, P., Farhadi, M., Dabbaghjamanesh, M., Jolfaei, A. and Sabahi, M., 2021. Fault current limiter dynamic voltage restorer (FCL-DVR) with reduced number of components. *IEEE Journal of Emerging and Selected Topics in Industrial Electronics*, *2*(4), pp.526-534.

[11] Aydogmus, O., Boztas, G. and Celikel, R., 2022. Design and analysis of a flywheel energy storage system fed by matrix converter as a dynamic voltage restorer. *Energy*, *238*, p.121687.

[12] Falehi, A.D. and Torkaman, H., 2021. Promoted supercapacitor control scheme based on robust fractional-order super-twisting sliding mode control for dynamic voltage restorer to enhance FRT and PQ capabilities of DFIG-based wind turbine. *Journal of Energy Storage*, *42*, p.102983.

[13] Ansal, V., 2020. ALO-optimized artificial neural network-controlled dynamic voltage restorer for compensation of voltage issues in distribution system. *Soft Computing*, *24*(2), pp.1171-1184.

[14] Chen, X.Y., Zhang, M.S., Jiang, S., Gou, H.Y., Xie, Q., Chen, Y. and Yang, R.H., 2021. An SMES-based current-fed transformerless series voltage restorer for DC-load protection. *IEEE Transactions on Power Electronics*, *36*(9), pp.9698-9703.

[15] Khan, M.A., Haque, A. and Kurukuru, V.B., 2021. Dynamic voltage support for low-voltage ride-through operation in single-phase grid-connected photovoltaic systems. *IEEE Transactions on Power Electronics*, *36*(10), pp.12102-12111.

[16] Silva, W.W.A., Oliveira, T.R. and Donoso-Garcia, P.F., 2020. An improved voltage-shifting strategy to attain concomitant accurate power sharing and voltage restoration in droop-controlled DC microgrids. *IEEE Transactions on Power Electronics*, *36*(2), pp.2396-2406.
[17] Han, Y., Ning, X., Li, L., Yang, P. and Blaabjerg, F., 2021. Droop coefficient correction control for power sharing and voltage restoration in hierarchical controlled DC microgrids. *International Journal of Electrical Power & Energy Systems*, *133*, p.107277.
[18] Yang, T., He, Y. and Liu, G.P., 2022. Distributed voltage restoration of AC microgrids under communication delays: A predictive control perspective. *IEEE Transactions on Circuits and Systems I: Regular Papers*, *69*(6), pp.2614-2624.
[19] Xing, L., Guo, F., Liu, X., Wen, C., Mishra, Y. and Tian, Y.C., 2020. Voltage restoration and adjustable current sharing for DC microgrid with time delay via distributed secondary control. *IEEE Transactions on Sustainable Energy*, *12*(2), pp.1068-1077.
[20] Effendy, M., Ashari, M. and Suryoatmojo, H., 2022. Load Sharing and Voltage Restoration Improvement in DC Microgrids with Adaptive Droop Control Strategy. *International Journal on Engineering Applications*, *10*(4), pp.233-240.
[21] Abas, N., Dilshad, S., Khalid, A., Saleem, M.S. and Khan, N., 2020. Power quality improvement using dynamic voltage restorer. IEEE Access, 8, pp.164325-164339.
[22] Babu, V., Ahmed, K.S., Shuaib, Y.M. and Manikandan, M., 2021. Power quality enhancement using dynamic voltage restorer (DVR)-based predictive space vector transformation (PSVT) with proportional resonant (PR)-controller. IEEE Access, 9, pp.155380-155392.
[23] Reddy, S.G., Ganapathy, S. and Manikandan, M., 2022. Power quality improvement in distribution system based on dynamic voltage restorer using PI tuned fuzzy logic controller. Электротехника и электромеханика, (1 (eng)), pp.44-50.
[24] Farooqi, A., Othman, M.M., Radzi, M.A.M., Musirin, I., Noor, S.Z.M. and Abidin, I.Z., 2022. Dynamic voltage restorer (DVR) enhancement in power quality mitigation with an adverse impact of unsymmetrical faults. Energy Reports, 8, pp.871-882.
[25] Prasad, D. and Dhanamjayulu, C., 2022. Solar PV integrated dynamic voltage restorer for enhancing the power quality under distorted grid conditions. Electric Power Systems Research, 213, p.108746.
[26] Nagarajan, L. and Senthilkumar, M., 2022. Power quality improvement in distribution system based on dynamic voltage restorer using rational energy transformative optimization algorithm. Journal of Electrical Engineering & Technology, 17(1), pp.121-137.
[27] Abdelkader, A.B., Mouloudi, Y. and Soumeur, M.A., 2023. Integration of renewable energy sources in the dynamic voltage restorer for improving power quality using ANFIS controller. Journal of King Saud University-Engineering Sciences, 35(8), pp.539-548.
[28] Abas, N., Dilshad, S., Khalid, A., Saleem, M.S. and Khan, N., 2020. Power quality improvement using dynamic voltage restorer. *IEEE Access*, *8*, pp.164325-164339.
[29] Sarker, K., Sarkar, K., Sarker, J., Bhowmik, P., Chatterjee, D. and Goswami, S.K., 2024. Power quality investigation with multilevel inverter by photovoltaic-fed dynamic voltage restorer. *International Journal of Modelling and Simulation*, pp.1-27.
[30] Deshpande, C.V., Chilipi, R. and Arya, S.R., 2024. Modified fractional least mean square-based control scheme for dynamic voltage restorer to improve power quality. *Electrical Engineering*, pp.1-19.

[31] Hubálovská, M., Hubálovský, Š. and Trojovský, P., 2024. Botox Optimization Algorithm: A New Human-Based Metaheuristic Algorithm for Solving Optimization Problems. *Biomimetics*, *9*(3), p.137.
[32] Shin, M., Lee, J. and Jeong, K., 2024. Estimating quantum mutual information through a quantum neural network. *Quantum Information Processing*, *23*(2), pp.1-16.